MR. CHUNCHUN LI (Orcid ID : 0000-0002-3657-5856)

MR. HUAICHENG XIANG (Orcid ID : 0000-0002-5967-8815)

Article type : Article

Phase formation and microwave dielectric properties of BiMVO5 (M = Ca, Mg) ceramics potential for LTCC application

Kai Cheng[1, 3], Chunchun Li[1, 2*], Huaicheng Xiang[1], Ying Tang[1], Yihua Sun[3], Liang Fang[1, 3*]

[1]*State Key Laboratory Breeding Base of Nonferrous metals and specific Materials Processing, Guangxi universities key laboratory of non-ferrous metal oxide electronic functional materials and devices, College of Material Science and Engineering, Guilin University of Technology, Guilin, 541004, China*

[2]*College of Information Science and Engineering, Guilin University of Technology, Guilin, 541004, China*

[3]*Key laboratory of inorganic nonmetallic crystalline and energy conversion materials, College of Materials and Chemical Engineering, Three Gorges University, Yichang, 443002, China*

---

[*] Corresponding Author, *lichunchun2003@126.com; fangliangg l001@aliyun.com*

This article has been accepted for publication and undergone full peer review but has not been through the copyediting, typesetting, pagination and proofreading process, which may lead to differences between this version and the Version of Record. Please cite this article as doi: 10.1111/jace.15943

This article is protected by copyright. All rights reserved.

Accepted Article

Accepted Article

Abstract

Two low-firing $BiMVO_5$ (M = Ca, Mg) ceramics were prepared in the sintering temperature range of 760-850 °C. Their differences in phase formation, sintering behavior, and dielectric performances were investigated. $BiCaVO_5$ formed a single phase with an orthorhombic structure, while $BiMgVO_5$ crystallized in a monoclinic structure that needs longer dwelling time to obtain single phase. The optimized microwave dielectric properties were obtained with $\varepsilon_r = 15.70$, $Q\times f = 55{,}000$ GHz (at 10.6 GHz), and $\tau_f = -71$ ppm/°C for $BiCaVO_5$, $\varepsilon_r = 18.55$, $Q\times f = 86{,}860$ GHz (at 9.63 GHz), and $\tau_f = -65$ ppm/°C for $BiMgVO_5$. Additionally, the large negative τ_f values of $BiMVO_5$ (M = Ca, Mg) ceramics were successfully adjusted by forming composite ceramics with $CaTiO_3$ and near-zero τ_f values of +2 ppm/°C and -3 ppm/°C were obtained in $0.92BiCaVO_5$-0.08CaTiO3 and $0.94BiMgVO_5$-$0.06CaTiO_3$, respectively. Both ceramics exhibited good chemical compatibility with Ag electrode. The results demonstrate $BiMVO_5$ (M = Ca, Mg) ceramics to be attractive candidates in LTCC technology.

Keywords: Ceramics; Microwave dielectric properties; LTCC; $BiMVO_5$

1. Introduction

Low temperature co-fired ceramics (LTCC) technology has attracted a great deal of attention due to its ability to fulfill the miniaturization and portability of microwave devices by integrating passive components within a monolithic bulk module [1-3]. Generally,

This article is protected by copyright. All rights reserved.

Accepted Article

microwave dielectric ceramics as substrates or microwave passive components in LTCC devices should possess a high quality factor ($Q\times f$), an appropriate permittivity (ε_r), and a near-zero temperature coefficient of resonance frequency (τ_f). In LTCC multilayer devices, alternating dielectric ceramics stack with internal metallic electrode layers where silver (Ag) is commonly used because of its high conductivity [4, 5]. In order to satisfy the co-firing with the electrode, the sintering temperature of the substrate materials is limited to be lower than the melting temperature of inner electrode (e.g., 960 °C for silver). Searching for novel low-firing materials with splendid dielectric properties is still of intriguing interest in view of scientific research and practical application. To date, a number of glass-free low-firing microwave dielectric ceramics with good performances have been reported and most of them are oxides based on low-melting constituents, such as V_2O_5-rich [6, 7], TeO_2-rich [8, 9], Bi_2O_3-rich [10, 11], MoO_3-rich oxide [12, 13]. It is proposed that the low melting-point constituents could facilitate the mass transport through liquid-phase sintering. Thus, this common feature opens up a way for the further development of low-firing ceramics to focus on the systems with low-melting constituents. Reasonably, material systems involving two or more low melting constituents are of value for developing low firing ceramics.

The Bi_2O_3-MO-V_2O_5 (M = Mg, Zn, Co, and Ni etc.) ternary system simultaneously contains two low-melting constituents, Bi_2O_3 (825 °C) and V_2O_5 (690 °C). Thus, this system is expected to have low sintering temperatures and promising microwave dielectric performances. The vanadates $BiMVO_5$ family in Bi_2O_3-MO-V_2O_5 system where M^{2+} can be Ca, Cd, Pb, Mg, Mn are analog of the paragonite mineral $BiNiAsO_5$ [14, 15]. Some $BiMVO_5$

This article is protected by copyright. All rights reserved.

Accepted Article

have recently been synthesized and characterized due to the expectation on their potential ferroelectric properties, nonlinear optical properties, and luminescent properties [16, 17], arising partly from the presence of the Bi^{3+} lone-pair electrons [18, 19]. In the present work, we focused on the $BiMVO_5$ system to explore novel low-firing microwave dielectric material. Two single-phase compounds $BiMgVO_5$ and $BiCaVO_5$ were obtained by optimizing the sintering conditions and the microwave dielectric properties were evaluated. Their structural difference was evaluated based on XRD, Rietveld refinement, and Raman spectroscopy analysis. Their chemical compatibility with metal electrodes was also studied.

2. Experimental Procedure

The $BiMVO_5$ (M = Ca, Mg) ceramics were prepared via solid-state reaction. Stoichiometric ratios of reagent-grade starting materials, Bi_2O_3 (> 99%, Guo-Yao Co. Ltd, Shanghai, China), $CaCO_3$ (> 99.99%, Guo-Yao Co. Ltd, Shanghai, China), MgO (> 99.99%, Guo-Yao Co. Ltd, Shanghai, China) and NH_4VO_3 (> 99%, Guo-Yao Co. Ltd, Shanghai, China) were mixed in a planetary ball-mill in a nylon jar for 6 h using zirconia balls as a grinding medium. The mixed slurries were dried and calcined at 750-900 °C (an interval of 50 °C) for 2-8 h. The calcined powders were subsequently ball-milled for 6 h again, dried, and the phase composition of which was analyzed using x-ray diffractometer. Thereby, the dried powders calcined at 750 °C/4 h for $BiCaVO_5$ and 750 °C/6 h for $BiMgVO_5$ were mixed with 5 wt% polyvinyl alcohol and pressed into cylindrical disks of 10 mm diameter and about 5 mm height at a pressure of about 200 MPa, respectively. The pellets were heated at 550 °C for 2 h to remove the organic binder. Subsequently, the pellets of $BiMVO_5$ (M = Ca, Mg)

This article is protected by copyright. All rights reserved.

Accepted Article

sintered at 760-850 °C for 6 h at a heating rate of 5 °C/min. Composite ceramics between $BiMVO_5$ (M = Ca, Mg) and $CaTiO_3$ were prepared with a general formula $(1-x)BiMVO_5-xCaTiO_3$ ($0 \leq x \leq 0.12$) to adjust the thermal stability. The calcined $BiMVO_5$ (M = Ca, Mg) powders were mixed with pure single phase $CaTiO_3$, ball milled for 6 h, and then pressed into pellets and sintered in the sintering range of 760-860 °C.

The phase composition of samples was analyzed using an x-ray diffractometer (Cu$K\alpha$1, 1.54059A, model X'pert PRO, PANalytical, Almelo, the Netherlands). The microstructure of the sintered samples was observed by scanning electron microscopy (SEM; Model JSM6380-LV, JEOL, Tokyo, Japan). The bulk densities of the sintered samples were measured by the Archimedes' method. The microwave dielectric properties were measured using a network analyzer (Model N5230A, Agilent Co., Palo Alto, Canada) and a temperature chamber (Delta 9039, Delta Design, San Diego, CA). The temperature coefficient of resonant frequency was measured in the temperature range from 25 °C (T_1) to 85 °C (T_2). The values were calculated as follows:

$$\tau_f = \frac{f_2 - f_1}{f_1(T_2 - T_1)} \tag{1}$$

where, f_1 and f_2 represent resonant frequencies at temperatures T_1 and T_2, respectively.

This article is protected by copyright. All rights reserved.

Accepted Article

3. Results and discussion

Fig. 1a_1 shows the XRD patterns of the $BiCaVO_5$ powders fired at 750 °C/4 h and $BiMgVO_5$ powders fired at 900 °C/4 h (Fig. 1a_2) and 750 °C/4 h (Fig. 1a_3). For $BiCaVO_5$, all the observed peaks were indexed according to the JCPDS card No. 81-1775 with an orthorhombic unit cell with *Pbca* (61) space group, indicating the formation of a single phase. However, it is clearly seen that $BiMgVO_5$ exhibited mixed phases with the main phase $BiMgVO_5$ (JCPDS No.72-9949) along with trace amount of $Bi_{4.2}Mg_{0.2}V_{1.6}O_{10.5}$ (JCPDS No.48-0267). Despite the fraction of $BiMgVO_5$ phase increased with increasing calcination temperature, but a substantial fraction of the second phase still remained. The fraction of $BiMgVO_5$ phase was evaluated approximately by the following equation [20],

$$BiMgVO_5\ (vol\%) = \frac{I_{A(-221)}}{I_{A(-221)} + I_{B(103)}} \times 100 \qquad (2)$$

where, I_A and I_B are the strongest lines of $BiMgVO_5$ (-221) and $Bi_{4.2}Mg_{0.2}V_{1.6}O_{10.5}$ (103) respectively. The relative amount of the $BiMgVO_5$ increased from 80% to 98% as the temperature of increased from 750 to 900 °C. It seems difficult to obtain single-phase $BiMgVO_5$ just simply raising the firing temperature. It is well accepted that the second phase(s) adversely affect the dielectric properties of microwave ceramics, especially the quality factor [21-23]. Thus, in order to get single-phase $BiMgVO_5$, efforts were made to change the preparation processes in terms of the soaking time. Fig. 1b shows the XRD patterns of the mixtures calcined at 750 °C with different soaking times. Obviously, the fraction of the second phase decreased as the soaking time increased, indicated by the decrease in the intensity of the reflection at $2\theta \sim 28.6^{o}$ and the pure $BiMgVO_5$ phase with a

This article is protected by copyright. All rights reserved.

monoclinic structure in $P2_1/n$ (14) space group was obtained when the holding time was lengthened to 6 h and 8 h. These results reveal that soaking time plays a more prominent role in the formation of single-phase $BiMgVO_5$ ceramic than sintering temperature.

It is worth noting that $BiCaVO_5$ and $BiMgVO_5$ crystallized in different crystal structures with regards to their diverse XRD patterns. In order to obtain a deeper insight into the structural differences, Rietveld refinement was performed based on the fine XRD data, as shown in Fig. 2a and Fig. 2b. A good match between the observed and calculated XRD patterns, and the acceptable low residual factors with R_{wp} = 8.32%, R_{exp} = 2.12% and R_p = 5.74% for $BiMgVO_5$ and R_{wp} = 6.97%, R_{exp} = 3.55% and R_p = 3.71% for $BiCaVO_5$ were obtained. The lattice parameters derived from the refinement are a = 7.5487(6) Å, b = 11.6163(7) Å, c = 5.3059(6) Å, $\alpha = \gamma = 90°$, β = 107.32813°, and V = 444.159 Å^3 (Z = 4), which were summarizd in Table 1. Fig. 2c and Fig. 2d show the schematic crystal structure of $BiCaVO_5$ and $BiMgVO_5$. The structure of $BiCaVO_5$ is characterized by the edge-linked [CaO_7] polyhedra layers, isolated VO_4 tetrahedra and interstitial Bi^{3+} with the asymmetric surrounding of oxygens [24-26]. The adjacent [CaO_7] polyhedra and [VO_4] tetrahedra are corner-linked. However, $BiMgVO_5$ is constructed by a three-dimensional network of two edge-sharing [MgO_6] octahedra that are corner-linked by [VO_4] tetrahedra, forming large tunnels along c-axis. The interstitial Bi^{3+} with asymmetric ambient oxygens locates in the tunnels and can also be described as Bi^{3+} combined with oxygen to form tilting [BiO_6] octahedra. The average tetrahedral distortion of the V-site was calculated (see in Table 1) using the following equation:

This article is protected by copyright. All rights reserved.

Accepted Article

Accepted Article

$$\Delta = \frac{1}{4}\sum\{\frac{R_i - R_{av}}{R_{av}}\} \tag{3}$$

R_i is the individual and R_{av} the average bond length of the oxygen tetrahedron. The average tetrahedral distortion of [VO_4] in $BiCaVO_5$ (1.46) is higher than that of $BiMgVO_5$ (1.34), reflecting their structural difference that would affect the dielectric properties.

The room-temperature Raman spectra of $BiMVO_5$ (M = Ca, Mg) are shown in Fig.3. The Raman active modes of the $BiCaVO_5$ and $BiMgVO_5$ were characterized using the group theoretical method according to the *Pbca* and *P2₁/n* space group, respectively, as follows:

$$\Gamma_{(BiCaVO5)} = 24\ A_g + 24\ B_{1g} + 24B_{2g} + 24B_{3g} \tag{4}$$

$$\Gamma_{(BiMgVO5)} = 24\ A_g + 24B_g \tag{5}$$

As shown in Fig. 3, the modes in the low-frequency region of 150-300 cm^{-1} could be attributed to the external modes, which involves the translational vibrations of the Ca^{2+}, Bi^{3+} and $[VO_4]^{3-}$ ions. For the modes between 300 cm^{-1} and 800 cm^{-1}, the bands were principally due to the bending and stretching vibrations of Bi-O bands, and four bands of them (319, 336, 359, 379 cm^{-1}) are associated with V-O bending vibrations. As for the 800-1000 cm^{-1} region of $BiCaVO_5$ Raman spectrum, it exhibits 3 bands (809, 832, 878 cm^{-1}), which corresponds to the internal stretching vibrations (Ag mode) of [VO_4] tetrahedra. Similarly, the four bands (116, 138, 190, 246 cm^{-1}) of the $BiMgVO_5$ were assigned to the translational vibrations of the

This article is protected by copyright. All rights reserved.

Mg^{2+}, Bi^{3+} and $[VO_4]^{3-}$. The vibrations of Bi-O bands and the bending vibrations of V-O occurred at 300-700 cm^{-1} and 700-1000 cm^{-1}, respectively. The different Raman modes and Raman shift of $BiCaVO_5$ and $BiMgVO_5$ reveal their different crystal structure.

SEM images of the $BiCaVO_5$ ceramic sintered at 760 °C to 850 °C for 6 h are shown in Fig. 4(a-e). As observed, a relatively porous microstructure consisting of small grains (approximately 1-3 μm) was observed in the 760 °C-sintered ceramic. With increasing sintering temperature, the number of pores decreased accompanied by an obvious grain growth. Densification occurred when sintered at 820 °C, characterized by a dense microstructure with distinct grain boundaries and homogeneous grains about 4 μm. However, when the temperature increased to 850 °C, large grains (~ 10 μm) appeared. Microstructural evolution as a function of sintering temperature in $BiMgVO_5$ was similar to $BiCaVO_5$ and a dense and uniform microstructure was developed in the sample sintered at 800 °C for 6 h, as shown in Fig. 4(f-j).

Fig. 5 plots the bulk density, relative density and microwave dielectric properties of the $BiCaVO_5$ and $BiMgVO_5$ ceramics sintered at various temperatures. In Fig. 5a_1 for $BiCaVO_5$, with increasing temperature the relative density firstly increased from 91.9% at 760 °C, reached a to a maximum value ~ 96.2% at 820 °C, and a further increase in sintering temperature decreased the relative density to 94.9% which was related to the exaggerated grain growth at elevated temperatures. As shown in Fig. 5a_2 the relative permittivity (ε_r) of

Accepted Article

This article is protected by copyright. All rights reserved.

$BiCaVO_5$ ceramics increased from 14.10 to 15.70 as the sintering temperature increased from 760 to 820 °C, and then slightly decreased, exhibiting a similar variation trend to the density. As for $BiMgVO_5$ (see in Fig. $5b_1$ and Fig. $5b_2$), the density of $BiMgVO_5$ also exhibited a similar variation trend with the sintering temperature but with a lower magnitude as compared with $BiCaVO_5$. The relative density of $BiMgVO_5$ sintered at the lower temperature 760 °C was high (95.1% of the theoretical density, ~5.45 g/cm^3), which was increased to 98.7% when sintered at 800 °C for 6 h. Additionally, slight variation in relative permittivity (18.20-18.50) of $BiMgVO_5$ is observed as the sintering temperature increased, which can be accounted for the high densification of the $BiMgVO_5$ specimens. In general, the relative permittivity depends on the several factors such as structural characteristics, ionic polarizability, the secondary phase, density, and defects, etc [27, 28]. In this work, the effects of the secondary phase on ε_r value were negligible, as no secondary phase was detected by the XRD within its accuracy. These results indicate that the density played a dominating role in the relative permittivity.

The theoretical permittivity is determined by the molecular polarizability and can be evaluated based on the Clausius-Mossotti equation [29, 30].

$$\varepsilon_{th} = \frac{3V + 8\pi\alpha}{3V - 4\pi\alpha} \tag{6}$$

where V is the cell volume. The theoretical permittivity was calculated to be 18.72 for $BiCaVO_5$ and 20.32 for $BiMgVO_5$. This can explain for the larger ε_r value of $BiMgVO_5$ than

This article is protected by copyright. All rights reserved.

Accepted Article

$BiCaVO_5$. In order to eliminate the influence of the porosity on dielectric permittivity, the Bosman and Having's correction equation was used: $\varepsilon_{corrected} = \varepsilon_r\,(1 + 1.5p)$, where p is the fractional porosity, $\varepsilon_{corrected}$ and ε_r are the corrected and measured relative permittivity, respectively. The $\varepsilon_{corrected}$ values, shown in Fig. 5a$_2$ and Fig. 5b$_2$, remained stable around 16.1 for $BiMgVO_5$ and 18.9 for $BiMgVO_5$ of different samples, accounting for the vital effect of density. On the other hand, it should be noted that the relative error between the corrected and theoretical permittivity is extremely high, 22.9% for $BiCaVO_5$ and 16.9% for $BiMgVO_5$. The large deviation indicates another factor affecting the relative permittivity, which can be attributed to the lone electron pair of bismuth [31, 32]. Similar results were also reported in other Bi-based ceramic systems [33, 34].

It is well known that the dielectric loss at microwave frequencies depends not only on the intrinsic losses caused by the lattice vibration but also on the extrinsic losses, e.g. densification, secondary phase, grain boundaries and grain sizes, defects, etc [35, 36]. As shown in Fig. 5a$_3$ and Fig. 5b$_3$, the variation in the $Q\times f$ value with the sintering temperature is similar to the density. As the sintering temperature increased from 760 °C to 820 °C, the $Q\times f$ value reached a maximum value ~ 55,000 GHz for $BiCaVO_5$, and ~ 86,860 GHz for $BiMgVO_5$ when sintered at 800 °C, which is related to the increased densification and homogeneous microstructure [37, 38]. Further increase in sintering temperature decreased the quality factor slightly, which might be explained by the microstructure degradation caused by the abnormal grain growth [39]. In addition, the higher $Q\times f$ value of $BiMgVO_5$ than $BiCaVO_5$ is also related to the higher densification of $BiMgVO_5$. Fig. 5a$_3$ and Fig. 5b$_3$ shows

This article is protected by copyright. All rights reserved.

Accepted Article

Accepted Article

the variation in the calculated packing fraction versus sintering temperature, which is consistent with the change in $Q\times f$ values of $BiMVO_5$ (M = Ca, Mg) ceramics. Therefore, the variation in $Q\times f$ value in $BiMVO_5$ (M = Ca, Mg) origins from the combined contributions from the relative density and the packing fraction. In contrast, the τ_f values of both ceramics were not affected significantly by the sintering temperature and remained stable around -71 ppm/°C for $BiCaVO_5$ and -65 ppm/°C for $BiMgVO_5$, as shown in Fig. 5a$_4$ and Fig. 5b$_4$.

Since the large negative τ_f values of $BiMVO_5$ (M = Ca, Mg) ceramics are unacceptable for practical applications, formation of composite ceramics using $CaTiO_3$ with a positive τ_f value ~ + 800 ppm/°C was utilized to improve the temperature stability of $BiMVO_5$. XRD patterns of $(1-x)BiMVO_5-xCaTiO_3$ (M = Ca, Mg) ceramics only revealed the peaks of $CaTiO_3$ (JCPDS No. 76-2400) and $BiMVO_5$ phase, suggesting that no chemical reaction occurred between $BiMVO_5$ (M = Ca, Mg) and $CaTiO_3$. Table 2 lists the microwave dielectric properties of the composite ceramics. As expected, the τ_f value changed from negative to positive with increasing x value. A near-zero temperature coefficient of resonant frequency τ_f ~ +2 ppm/°C was achieved in $0.92BiCaVO_5-0.08CaTiO_3$ ceramic at 850 °C, along with ε_r ~ 17.63 and $Q\times f$ ~ 43,600 GHz. In addition, excellent combined microwave dielectric properties with a near-zero temperature coefficient of resonant frequency τ_f~ -3 ppm/°C and ε_r ~ 20.89 and a $Q\times f$ ~ 69,800 GHz was also obtained at $0.94BiCaVO_5-0.06CaTiO_3$ composition when sintered at 860 °C.

This article is protected by copyright. All rights reserved.

Chemical compatibility with inner electrodes is another important factor for the practical application. 20 wt % Ag powders were added to the $BiMVO_5$ (M = Ca, Mg) matrix and co-fired at 820 ^oC for 2 h to assess the chemical compatibility of $BiMVO_5$. The corresponding powder XRD profiles of the co-fired sample are shown in Fig. 7(a). The patterns of pure $BiMVO_5$ (M = Ca, Mg) are also given for comparison. Only peaks of Ag (JCPDS No. 89-3722) and $BiMVO_5$ phases were observed, indicating that after cofiring $BiMVO_5$ phase coexisted with silver electrodes, respectively. Backscattered electron image (BSE), energy-dispersive spectroscopy (EDS) analysis, and element mapping of the co-fired $BiCaVO_5$ ceramic are shown in Fig. 7(b). Two distinct kinds of grains were detected in BSE image. The large grains marked with "+1" are rich in silver, which was further confirmed by the element mapping. In addition, to further confirm the thermal expansion matching and interdiffusion between $BiMVO_5$ (M = Ca, Mg) ceramics sheet with Ag film, co-firing were conducted at 820 ^oC. As shown in Fig. 7, SEM micrographs and line scanning analysis on the fracture surface demonstrate distinct interfaces and no interdiffusion occurred between the layers of $BiMVO_5$ and Ag electrode. This results also illustrate good chemical and sintering shrinkage compatibilities among the $BiMVO_5$ matrix phases and Ag thick film, which is critical for the LTCC application.

In summary, $BiMVO_5$ (M = Ca, Mg) microwave dielectric ceramics were prepared at relatively low temperatures and their dielectric performances were characterized at microwave frequency band. Contrast to $BiCaVO_5$ being readily formed, longer dwelling time were required to obtain single phase $BiMgVO_5$, which were explained by their structural

Accepted Article

This article is protected by copyright. All rights reserved.

Accepted Article

difference being characterized by tetrahedral distortion. Their different dielectric properties were analyzed in terms of molecular polarizability, packing fraction. Besides, chemical compatibility with Ag electrode was verified based on XRD, SEM, EDS and elements mapping. This work shed lights on the exploitation of novel low-firing ceramics with promising microwave dielectric performances.

Acknowledgments

This work was financed by Natural Science Foundation of China (Nos. 51502047, 21561008, and 21761008), Natural Science Foundation of Guangxi Zhuang Autonomous Region (Nos. 2015GXNSFFA139003, 2016GXNSFBA380134, and 2016GXNSFAA380018), Project of Scientific Research and Technical Exploitation Program of Guilin (2016010702-2 and 20170225), and the State Scholarship fund of the China Scholarship Council (CSC201708420285). Author C.C. Li gratefully acknowledges the Guangxi Scholarship Fund of Guangxi Education Department.

References

1. Sebastian MT, Jantunen H. Low loss dielectric materials for LTCC applications: a review. Int Mate Rev. 2008; 53:57–90.

2. Reaney IM, Iddles D. Microwave dielectric ceramics for resonators and filters in mobile phone networks. J Am Ceram Soc. 2010; 89:2063–2072.

This article is protected by copyright. All rights reserved.

Accepted Article

3. Sebastian MT, Ubic R, Jantunen H. Microwave materials and applications, John Wiley & Sons. 2017.
4. Tseng CF, Tseng PJ, Chang CM, Kao YC. Novel temperature stable Li_2MnO_3 microwave dielectric ceramics with high Q for LTCC applications. J Am Ceram Soc. 2014; 97:1918–1922.
5. Lei W, Lu WZ, Zhu JH, Wang XH. Microwave dielectric properties of $ZnAl_2O_4$-TiO_2 spinel-based composites. Mater Lett. 2007; 61:4066–4069.
6. Wang Y, Zuo RZ. A novel low-temperature fired microwave dielectric ceramic $BaMg_2V_2O_8$ with ultra-low loss. J Eur Ceram Soc. 2016; 36:247–251.
7. Umemuraa R, Ogawa H, Ohsato H, Kana A, Yokoi A. Microwave dielectric properties of low-temperature sintered $Mg_3(VO_4)_2$ ceramic. J Am Ceram Soc. 2005; 25:2865–2870.
8. Kwon DK, Lanagan MT, Shrout TR. Microwave dielectric properties of BaO-TeO_2, binary compounds. Mater Lett. 2007; 61:1827–1831.
9. Udovic M, Valant M, Suvorov D. Phase formation and dielectric characterization of the Bi_2O_3-TeO_2 system prepared in an oxygen atmosphere. J Am Ceram Soc. 2010; 87;591–597.
10. Ma XH, Kweon SH, Nahm S, Kang CY, Yoon SJ, Kim YS. Synthesis and microwave dielectric properties of $Bi_2Ge_3O_9$ ceramics for application as advanced ceramic substrate. J Eur Ceram Soc. 2017; 37:605–610.

This article is protected by copyright. All rights reserved.

11. Zhou D, Wang H, Pang LX, Randall CA, Yao X. Bi_2O_3-MoO_3 binary system: an alternative ultralow sintering temperature microwave dielectric. J Am Ceram Soc. 2009; 92:2242–2246.

12. Zhang GQ, Guo J, Wang H. Ultra-low temperature sintering microwave dielectric ceramics based on Ag_2O-MoO_3 binary system. J Am Ceram Soc. 2017; 100:2604–2611.

13. Li CC, Wen WX, Xiang HC, Fang L, Sun YH. Low temperature sintering and microwave dielectric properties of $Zn_3Mo_2O_9$ ceramic. J Mater Sci -Mater Electron. 2018; 29:1907–1913.

14. Roberts AC, Burns PC, Gault RA, Criddle AJ, Feinglos MN, Stirling JAR. Paganoite, $NiBi^{3+}As^{5+}O_5$, a new mineral from johanngeorgenstadt, saxony, Germany: description and crystal structure. Eur J Mineral. 2001; 13:167–175.

15. Aliev A, Kozin MS, Colmont M, Siidra OI, Krivovichev SV, Mentré O. Synthesis, crystal structure, high-temperature behavior and magnetic properties of $CoBiO(AsO_4)$, a Co analogue of paganoite. Phys Chem Miner. 2015; 42:1–8.

16. Pei Z, Dijken AV, Vink A, Blasse G. Luminescence of calcium bismuth vanadate ($CaBiVO_5$). J Alloys Compd. 1994; 204:243–246.

17. Benmokhtar S, Jazouli AE, Chaminade JP, Gravereau P, Guillen F, Wall D. Synthesis, crystal structure and optical properties of $BiMgVO_5$. J Solid State Chem. 2004; 177:4175–4182.

Accepted Article

This article is protected by copyright. All rights reserved.

Accepted Article

18. Giraud S, Mizrahi A, Drache M, Conflant P, Winacourt JP, Steinfink H. A new family of compounds with tetrahedral anions: $Pb_nBiO_nXO_4$, X = V, P, As, n = 1, 2, 4, a comparison with lead oxysulfates $Pb_nPbO_n(SO_4)$. Solid State Sci. 2001; 3:593–602.

19. Pushkin DV, Serezhkin VN, Davidovich RL, Hu SZ. Stereochemical effect of a lone electron pair in the structure of diamine complexonates of bismuth(III). Russ J Inorg Chem. 2003; 48:700–704.

20. Reaney IM, Iddles D. Microwave dielectric ceramics for resonators and filters in mobile phone networks. J Am Ceram Soc. 2010; 89:2063–2072.

21. Chen YC, Weng MZ, Chang KC. Effect of sintering temperature and time on microwave dielectric properties of $CaNb_2O_6$ ceramics. J Mater Sci -Mater Electron. 2014; 25:44–851.

22. Luo WJ, Li LX, Yu SH, Sun Z, Zhang BW, Xia F. Structural, raman spectroscopic and microwave dielectric studies on high-Q materials in Ge-doped $ZnTiNb_2O_8$ systems. J Alloys Compd. 2018; 741:969–974.

23. Ogawa H, Yokoi A, Umemura R, Kan A. Microwave dielectric properties of $Mg_3(VO_4)_2$-$xBa_3(VO_4)_2$ ceramics for LTCC with near zero temperature coefficient of resonant frequency. J Eur Ceram Soc. 2007; 27:3099–3104.

24. Olchowka J, Colmont M, Kabbour H, Mentré O. Bismuth and vanadate activators in $BiMVO_5$ (M = Ca, Mg, Cd) phases: structural, electronic and optical specificities. J Alloys Compd. 2017; 709:373–380.

This article is protected by copyright. All rights reserved.

Accepted Article

25. Ketatni M, Abraham F, Mentre O. Channel structure in the new $BiCoPO_5$. comparison with $BiNiPO_5$. crystal structure, lone pair localisation and infrared characterization. Solid State Sci. 1999; 1:449–460.

26. Abraham F, Cousin O, Mentre O, Ketatni EM. Crystal structure approach of the disordered new compounds $BiB_{1.2}MB_{1.2}PO_{5.5}$ (M = Mn, Co, Zn): the role of oxygen-centered tetrahedra linkage in the structure of bismuth transition metal oxy-phosphates. J Solid State Compd. 2002; 167:168–181.

27. Li CC, Xiang HC, Xu MY, Tang Y, Fang L. Li_2AGeO_4 (A = Zn, Mg): Two novel low-permittivity microwave dielectric ceramics with olivine structure. J Eur Ceram Soc. 2018; 38:1524–1528.

28. Li CC, Xiang HC, Xu MY, Khaliq J, Chen JQ, Fang L. Low-firing and temperature stable microwave dielectric ceramics: $Ba_2LnV_3O_{11}$ (Ln = Nd, Sm), J Am Ceram Soc. 2018; 101: 773–781.

29. Shannon RD. Dielectric polarizabilities of ions in oxides and fluorides. J Appl Phys. 1993; 73:348–366.

30. Yoon SH, Kim DW, Cho SY, Hong KS. Investigation of the relations between structure and microwave dielectric properties of divalent metal tungstate compounds. J Eur Ceram Soc. 2006; 26:2051–2054.

31. Avdeev GV, Milenov TI, Egorysheva AV, Petrow KP, Skorikov VM. Crystal structure of $Bi_{36}MgP_2O_{60}$–delta. Russ J Inorg Chem. 2011; 56:913–918.

This article is protected by copyright. All rights reserved.

32. Pushkin DV, Sokolova EA, Serezhkin VN. BiO(n) coordination polyhedrons in crystal structures. Russ J Coord Chem. 2000; 26:1–5.

33. Luo H, Li J, Xu JG, Fang L, Tang Y, Li CC. A novel low-firing $BiZn_2VO_6$ microwave dielectric ceramic with low loss. J Mater Sci -Mater Electron. 2016; 27:210–214.

34. Li CC, Xiang HC, Luo H, Tang Y. Fang L. Characterization and microwave dielectric properties of $BiCa_2VO_6$ ceramic. J Mater Sci -Mater Electron. 2015; 26:9546–9551.

35. Joung MR, Kim JS, Song ME, Nahm S, Paik JH. Formation process and microwave dielectric properties of the $R_2V_2O_7$ (R = Ba, Sr, and Ca) ceramics. J Am Ceram Soc. 2009; 92:3092–3094.

36. Joung MR, Kim JS, Song ME, Nahm S, Paik JH, Choi BH. Formation and microwave dielectric properties of the $Mg_2V_2O_7$ ceramics. J Am Ceram Soc. 2009; 92:1621–1624.

37. Bi JX, Niu YJ, Wu HT. $Li_4Mg_3Ti_2O_9$: A novel low-loss microwave dielectric ceramic for LTCC applications. Ceram Int. 2017; 43:7522–7530.

38. Xiang HC, Li CC, Fang WS, Tang Y, Li CC. A novel low-firing microwave dielectric ceramic $Li_2ZnGe_3O_8$ with cubic spinel structure. J Eur Ceram Soc. 2017; 37:625–629.

39. Xiang HC, Li CC, Tang Y, Fang L. Two novel ultralow temperature firing microwave dielectric ceramics LiMVO6 (M = Mo, W) and their chemical compatibility with metal electrodes. J Eur Ceram Soc. 2017; 37:3959–3963.

Accepted Article

This article is protected by copyright. All rights reserved.

Accepted Article

Table 1 Crystallographic data obtained from Rietveld refinement and the distortion of [VO_4] tetrahedra for $BiMVO_5$ (M = Ca, Mg)

composition	Lattice parameters (Å)			R_{wp} (%)	R_p (%)	X^2 (%)	$\Delta_{[VO4]}$
	a	*b*	*c*				
$BiCaVO_5$	11.2022	5.4283	15.5605	6.97	3.71	3.55	1.46
$BiMgVO_5$	7.54876	11.61637	5.30596	8.32	5.74	2.12	1.34

Table 2 Microwave dielectric properties of (1-x)$BiMVO_5$-x$CaTiO_3$ (M = Ca, Mg) composite ceramic.

composition	x value	S.T. (^oC)	ε_r	$Q\times f$ (GHz)	τ_f (ppm/°C)
$BiCaVO_5$	0	820	15.70 ± 0.1	55,000 ± 2000	-71 ± 2.1
	0.04	830	16.56 ± 0.1	49,850 ± 1500	-31 ± 1.5
	0.08	850	17.63 ± 0.1	43,600 ± 1800	+2 ± 0.5
	0.12	880	19.40 ± 0.1	38,100 ± 2000	+22 ± 2.5
$BiMgVO_5$	0	820	18.50 ± 0.1	86,860 ± 1500	-65 ± 2.1
	0.03	840	19.15 ± 0.1	78,400 ± 1500	-38 ± 2.0
	0.06	860	20.89 ± 0.1	69,800 ± 1500	-3 ± 0.2
	0.09	880	22.05 ± 0.1	62,350 ± 1500	+11 ± 1.5

This article is protected by copyright. All rights reserved.

Accepted Article

Figure Captions:

Fig. 1 The XRD patterns of $BiMVO_5$ (M = Ca, Mg): (a_1): $BiCaVO_5$ calcined at 750 ^oC for 4 h, (a_2) calcined at 750 and (a_3) 900 ^oC for 4 h for $BiMgVO_5$; (b): $BiMgVO_5$ calcined at 750 °C as the sintering time varied from 2 to 8 h.

Fig. 2 The observed and calculated XRD patterns from Rietveld refinements and the crystal structure of $BiMVO_5$ (M = Ca, Mg).

Fig. 3 Raman spectrum of $BiMVO_5$ (M = Ca, Mg) ceramics sintered at 820 °C and 800 °C, respectively.

Fig. 4 The FE-SEM images of the $BiMVO_5$ (M = Ca, Mg) ceramics at various conditions (a-e):760, 780, 800, 820, 850 °C for $BiCaVO_5$, (f-j): 760, 780, 800, 820, 850 °C for $BiMgVO_5$.

Fig. 5 The bulk density, relative densities, packing fraction and the microwave dielectric properties (ε_r, $Q\times f$ and τ_f values) of the $BiMVO_5$ (M = Ca, Mg) ceramics sintered at various temperature for 6 h.

This article is protected by copyright. All rights reserved.

Accepted Article

Fig. 6 XRD patterns of the $0.92BiCaVO_5$-$0.08CaTiO_3$ ceramic sintered at 850 °C, and the $0.94BiMgVO_5$-$0.06CaTiO_3$ ceramic sintered at 860 °C.

Fig. 7 (a) Powder XRD patterns of the $BiMVO_5$ (M = Ca, Mg) ceramics co-fired with 20 wt % Ag at 820 °C. SEM images and corresponding EDS analysis of fracture surface of $BiMVO_5$ ceramic pellets co-fired with Ag electrode at 820 °C/2 h in air. (b) Backscattered electron image (BSE), energy-dispersive spectroscopy (EDS) analysis, and element mapping of the co-fired $BiCaVO_5$ ceramic.

This article is protected by copyright. All rights reserved.

Accepted Article

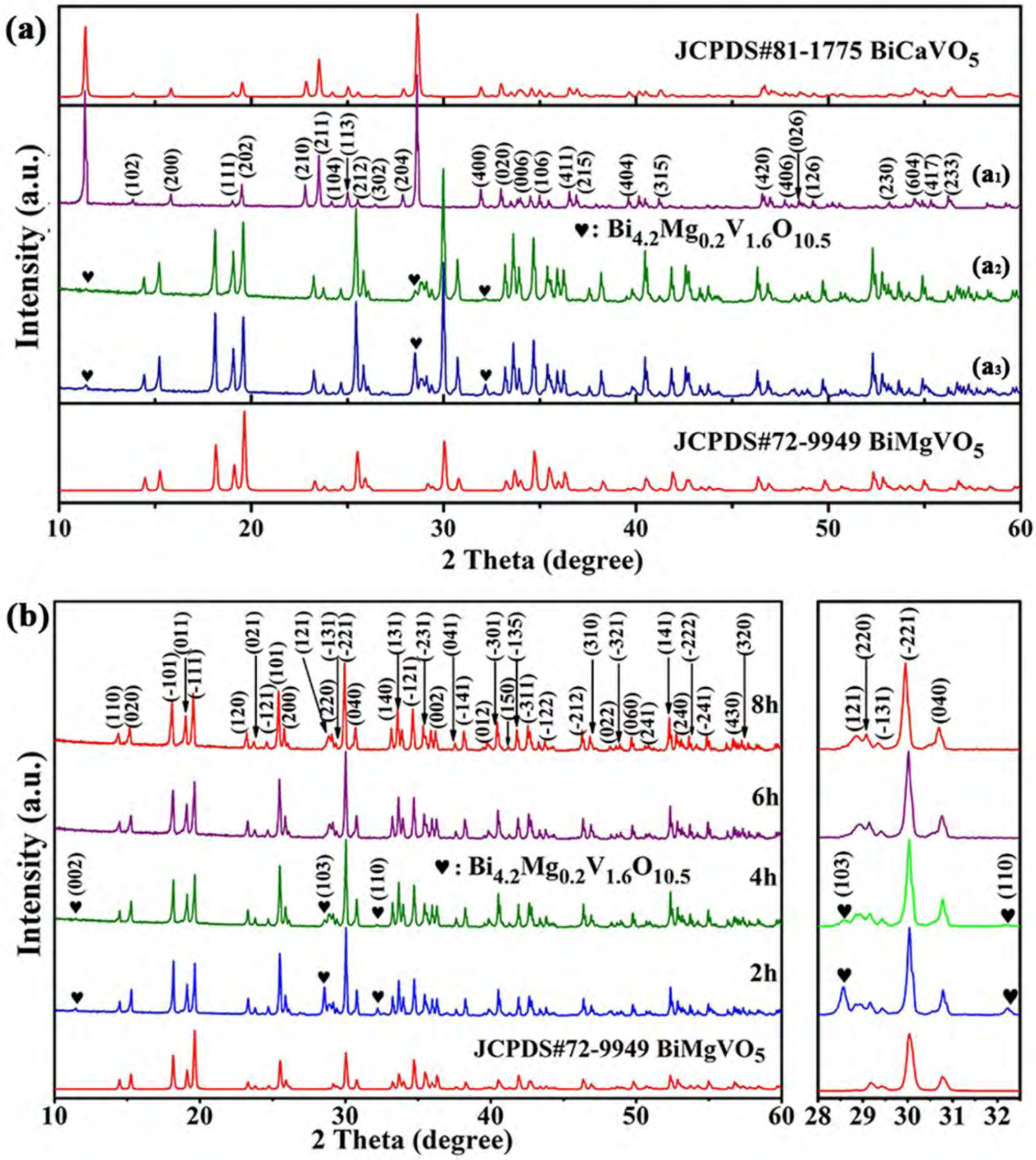

This article is protected by copyright. All rights reserved.

Accepted Article

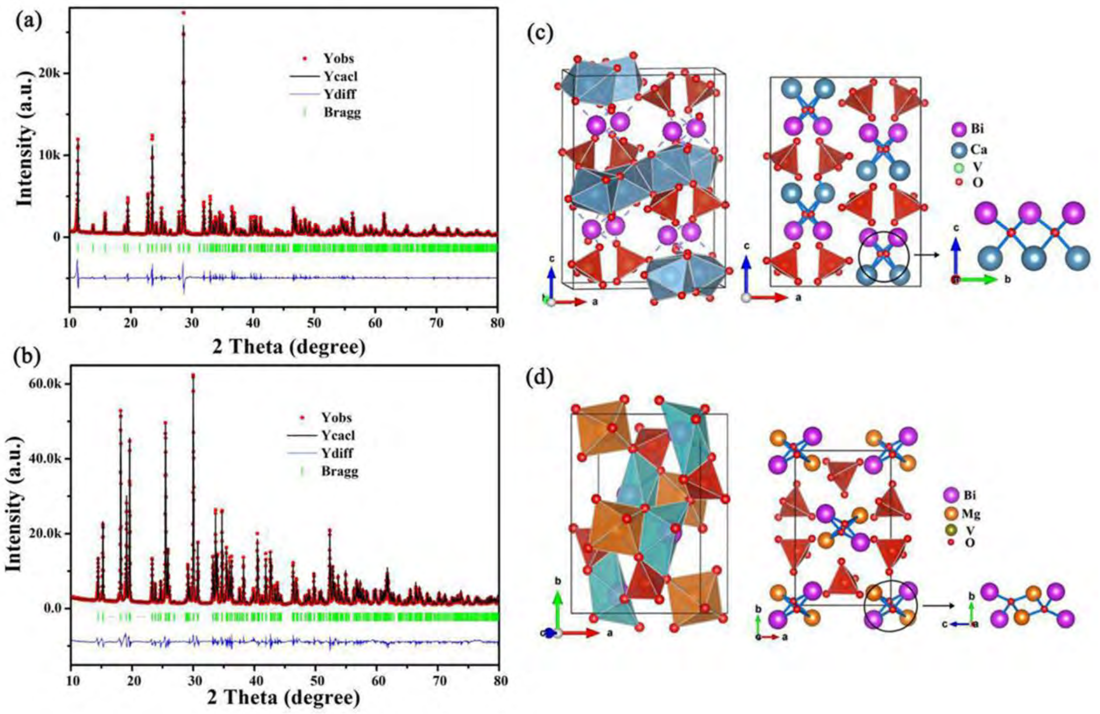

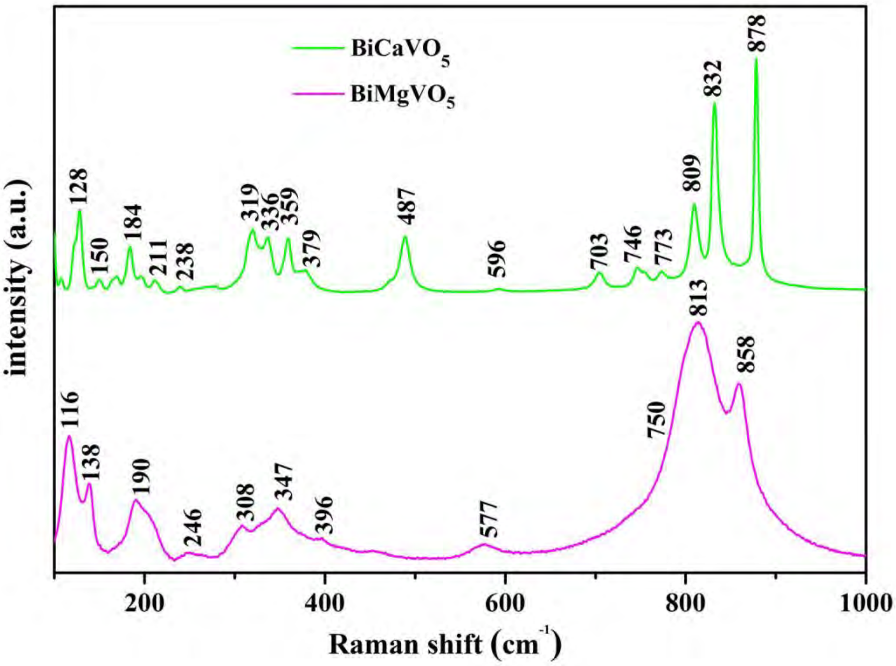

This article is protected by copyright. All rights reserved.

Accepted Article

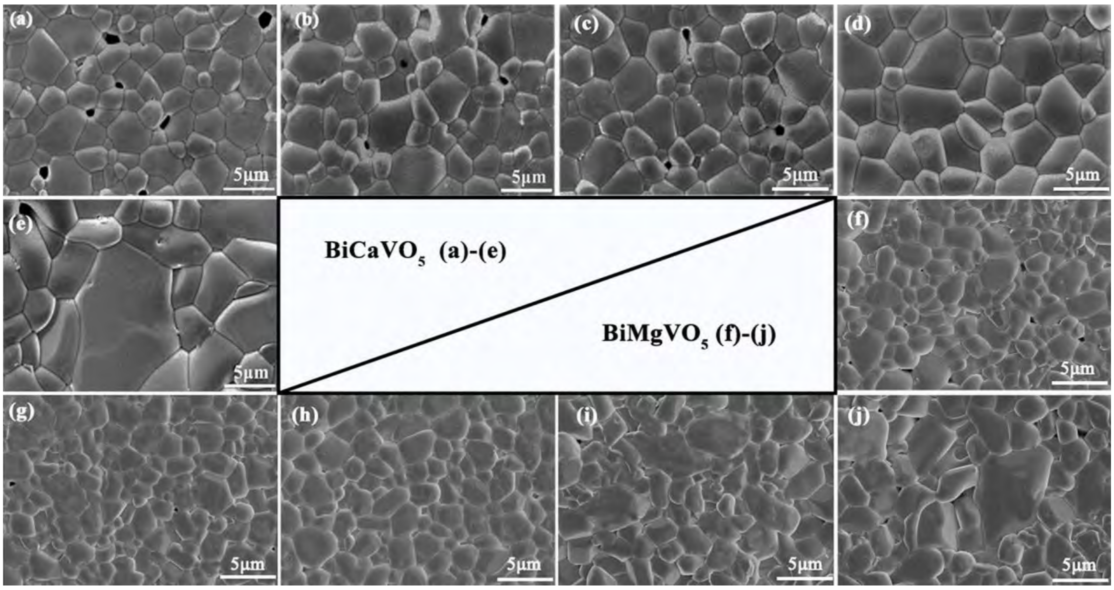

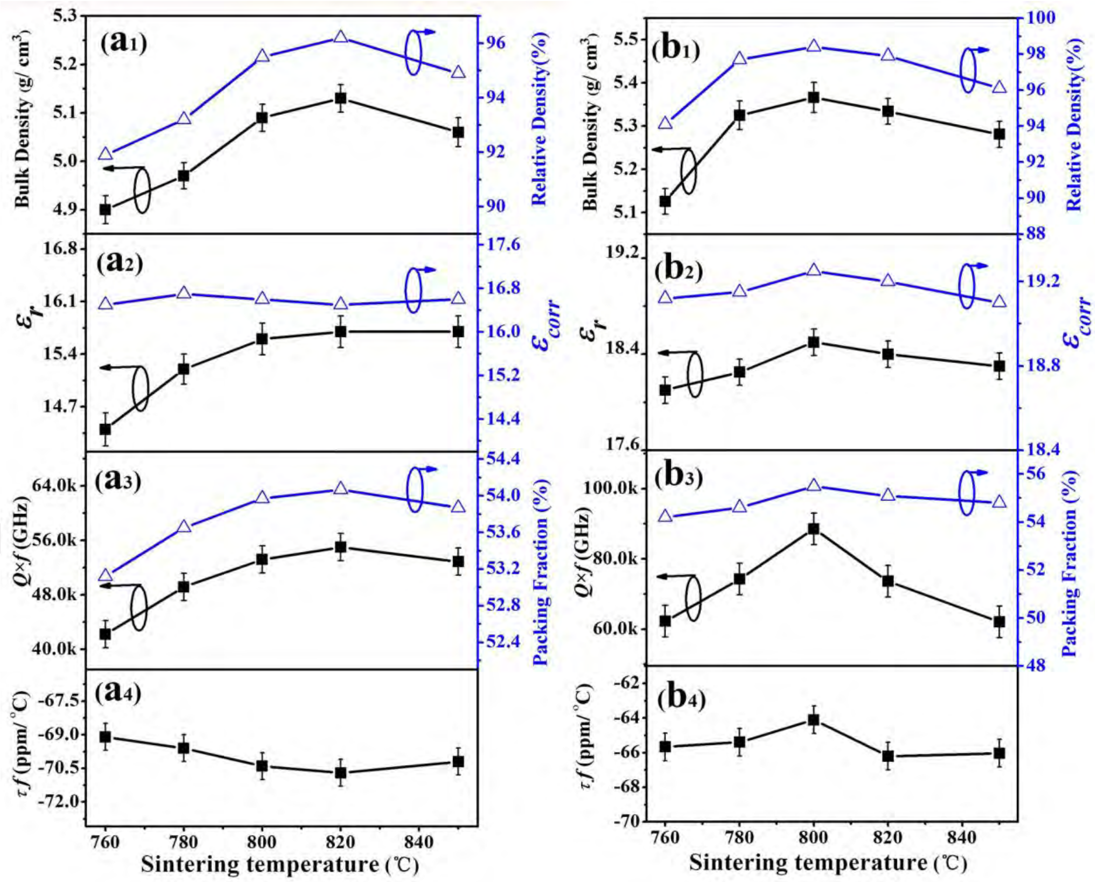

This article is protected by copyright. All rights reserved.

Accepted Article

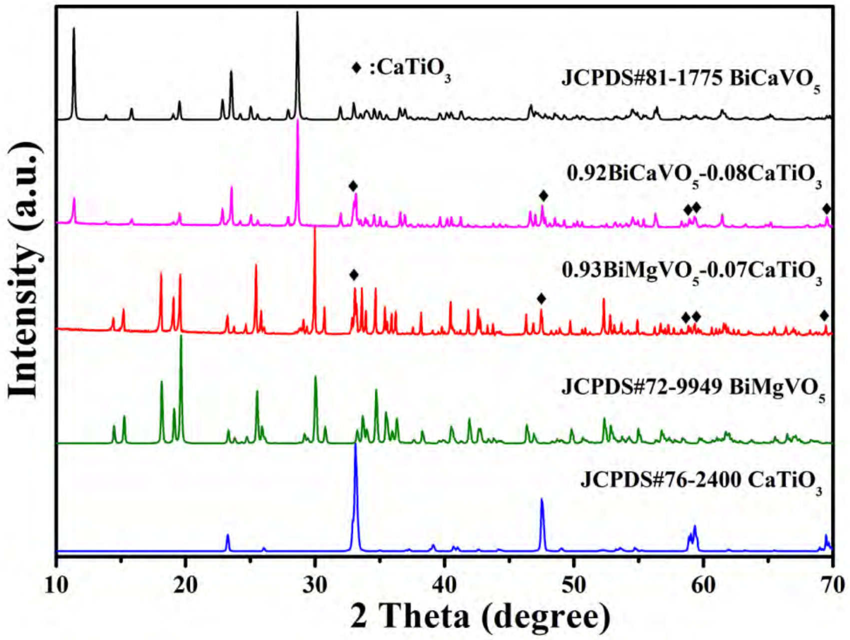

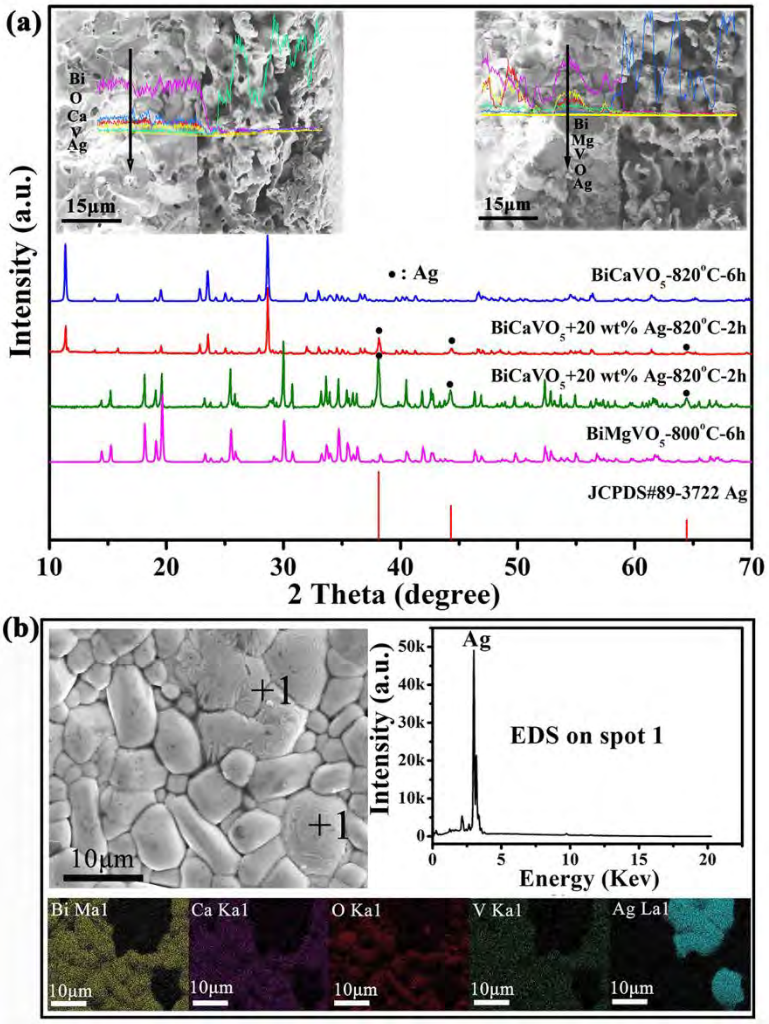

This article is protected by copyright. All rights reserved.